

NUCLEAR EFFECTS IN COHERENT
PHOTOPRODUCTION OF HEAVY QUARKONIA*

J. NEMCHIK

Czech Technical University in Prague, FNSPE
Břehová 7, 11519 Prague, Czech Republic
and

Institute of Experimental Physics SAS, Watsonova 47, 04001 Košice, Slovakia

B.Z. KOPELIOVICH

Departamento de Física, Universidad Técnica Federico Santa María
Avenida España 1680, Valparaíso, Chile*Received 29 November 2022, accepted 6 December 2022,
published online 25 May 2023*

Coherent photoproduction of heavy quarkonia on nuclear targets is studied within the QCD color dipole formalism including several main phenomena: (i) The correlation between the impact parameter of a collision \vec{b} and dipole orientation \vec{r} ; (ii) The higher-twist nuclear shadowing related to the QQ Fock state of the photon; (iii) The leading-twist gluon shadowing corresponding to higher Fock components of the photon containing gluons; (iv) Reduced effects of quantum coherence in a popular Balitsky–Kovchegov equation compared to calculations, which are frequently presented in the literature. Our calculations of differential cross sections are in good agreement with the recent ALICE data on charmonium production in ultra-peripheral nuclear collisions. We present also predictions for coherent photoproduction of other quarkonium states ($\psi'(2S)$, $\Upsilon(1S)$, and $\Upsilon'(2S)$) that can be verified by future measurements at the LHC.

DOI:10.5506/APhysPolBSupp.16.5-A7

* Presented at the Diffraction and Low- x 2022 Workshop, Corigliano Calabro, Italy, 24–30 September, 2022.

1. Significance of \vec{b} – \vec{r} correlation

The dipole–nucleon electroproduction amplitude within the *color dipole formalism* has the following factorized form [1]:

$$\mathcal{A}^N(x, \vec{q}) = 2 \int d^2b e^{i\vec{q}\vec{b}} \int d^2r \int_0^1 d\alpha \Psi_V^*(\vec{r}, \alpha) \mathcal{A}_{\bar{Q}Q}^N(\vec{r}, x, \alpha, \vec{b}) \Psi_{\gamma^*}(\vec{r}, \alpha, Q^2), \quad (1)$$

where \vec{q} is the transverse component of the momentum transfer, α is the fractional light-front (LF) momentum carried by a heavy quark or antiquark of the $\bar{Q}Q$ Fock component of the photon with the transverse separation \vec{r} .

The dipole–proton amplitude in Eq. (1), $\mathcal{A}_{\bar{Q}Q}^N(\vec{r}, x, \alpha, \vec{b})$, depends also on the impact parameter of collision \vec{b} . The LF distribution functions $\Psi_{\gamma^*}(\vec{r}, \alpha, Q^2)$ and $\Psi_V(\vec{r}, \alpha)$ correspond to transitions $\gamma^* \rightarrow \bar{Q}Q$ and $\bar{Q}Q \rightarrow V$, respectively.

Higher Fock components containing gluons contribute by default to the dipole–proton amplitude. Considering nuclear targets, these components must be taken into account *separately* due to different *coherence effects* in gluon radiation.

The essential feature of $\mathcal{A}_{\bar{Q}Q}^N(\vec{r}, x, \alpha, \vec{b})$ is the \vec{b} – \vec{r} correlation [1]

$$\begin{aligned} \text{Im } \mathcal{A}_{\bar{Q}Q}^N(\vec{r}, x, \alpha, \vec{b}) &= \frac{\sigma_0}{8\pi\mathcal{B}(x)} \left\{ \exp \left[-\frac{[\vec{b} + \vec{r}(1-\alpha)]^2}{2\mathcal{B}(x)} \right] \right. \\ &+ \exp \left[-\frac{(\vec{b} - \vec{r}\alpha)^2}{2\mathcal{B}(x)} \right] - 2 \exp \left[-\frac{r^2}{R_0^2(x)} - \frac{[\vec{b} + (1/2 - \alpha)\vec{r}]^2}{2\mathcal{B}(x)} \right] \left. \right\}, \quad (2) \end{aligned}$$

where the interaction vanishes if $\vec{r} \perp \vec{b}$ and reaches maximal strength if $\vec{r} \parallel \vec{b}$.

From the known amplitude (1), one can calculate the differential cross section

$$\frac{d\sigma^{\gamma N \rightarrow VN}(x, t = -q^2)}{dt} = \frac{1}{16\pi} |\mathcal{A}^N(x, \vec{q})|^2, \quad (3)$$

where $x = (M_V^2 + Q^2)/(W^2 + Q^2 - m_N^2)$ with the quarkonium mass M_V .

The real part of the $\gamma^*N \rightarrow VN$ amplitude and the skewness correction have been incorporated as described in Ref. [2].

As an example, Fig. 1 nicely demonstrates a manifestation of the \vec{b} – \vec{r} correlation in $\psi'(2S)$ -to- $J/\psi(1S)$ ratio of differential cross sections [1]. The

model predictions (solid line) are significantly different from results based on the standard assumption $\vec{b} \parallel \vec{r}$, frequently used in the literature. However, treating nuclear targets, the effect of the \vec{b} - \vec{r} correlation is diluted [3].

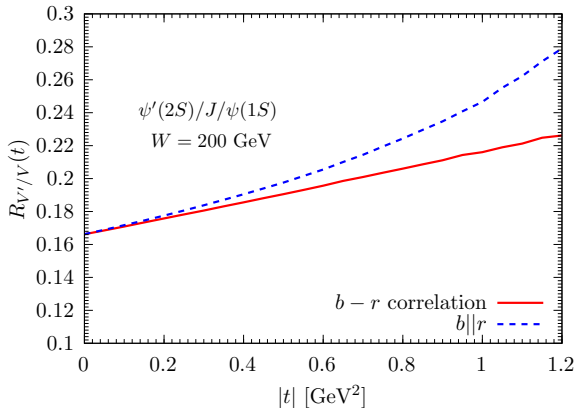


Fig. 1. Demonstration of the importance of $\vec{b}-\vec{r}$ correlation in photoproduction of the $\psi'(2S)$ -to- $J/\psi(1S)$ ratio of differential cross sections (3) at $W = 200$ GeV.

2. Higher-twist nuclear shadowing

The lowest Fock component of the projectile photon $|\bar{Q}Q\rangle$ has a small transverse dipole size $\propto 1/m_Q$, where m_Q denotes the heavy-quark mass. The corresponding shadowing correction is small as well since it is $\propto 1/m_Q^2$, and so it can be treated as a *higher twist effect*.

For the amplitude of coherent quarkonium electroproduction on nuclear targets, $\gamma^*A \rightarrow VA$, one can employ the above expression (1) for $\mathcal{A}^N(x, \vec{q})$, but replacing the dipole–nucleon by dipole–nucleus amplitude,

$$\mathcal{A}^A(x, \vec{q}) = 2 \int d^2b_A e^{i\vec{q}\cdot\vec{b}_A} \int d^2r \int_0^1 d\alpha \Psi_V^*(\vec{r}, \alpha) \mathcal{A}_{Q\bar{Q}}^A(\vec{r}, x, \alpha, \vec{b}_A) \Psi_{\gamma^*}(\vec{r}, \alpha, Q^2), \quad (4)$$

where b_A is the nuclear impact parameter.

In ultra-peripheral collisions (UPC) at the LHC, the photon virtuality $Q^2 \sim 0$, and the photon energy in the target rest frame is sufficiently high, so *the coherence length* exceeds substantially the nuclear radius R_A ,

$$l_c^{\bar{Q}Q} = 1/q_L = \frac{W^2 + Q^2 - m_N^2}{m_N(M_V^2 + Q^2)} \Big|_{Q^2 \sim 0} \approx \frac{W^2}{m_N M_V^2} \gg R_A.$$

Then fluctuations of the dipole size are frozen due to Lorentz time dilation and one can rely on *the eikonal form* for the dipole–nucleus partial amplitude at impact parameter \vec{b}_A

$$\begin{aligned} & \operatorname{Im} \mathcal{A}_{\bar{Q}Q}^A(\vec{r}, x, \alpha, \vec{b}_A) \Big|_{l_c^{\bar{Q}Q} \gg R_A} \\ &= 1 - \left[1 - \frac{1}{A} \int d^2b \operatorname{Im} \mathcal{A}_{\bar{Q}Q}^N(\vec{r}, x, \alpha, \vec{b}) T_A(\vec{b}_A + \vec{b}) \right]^A. \end{aligned} \quad (5)$$

Here, $T_A(\vec{b}_A) = \int_{-\infty}^{\infty} dz \rho_A(\vec{b}_A, z)$ is the nuclear thickness functions normalized as $\int d^2b_A T_A(\vec{b}_A) = A$, and $\rho_A(\vec{b}_A, z)$ is the nuclear density.

The corresponding expression for the differential cross section in the $l_c^{\bar{Q}Q} \gg R_A$ limit is analogous to that for proton, Eq. (3), and reads

$$\frac{d\sigma^{\gamma^*A \rightarrow VA}(x, t = -q^2)}{dt} \Big|_{l_c^{\bar{Q}Q} \gg R_A} = \frac{1}{16\pi} |\mathcal{A}^A(x, \vec{q})|^2. \quad (6)$$

3. Leading-twist gluon shadowing

The gluon shadowing (GS) corrections are related to the *higher Fock components* of the photon containing, besides the $\bar{Q}Q$ pair, additional gluons, $|\bar{Q}Qg\rangle$, $|\bar{Q}Q2g\rangle$, \dots , $|\bar{Q}Qng\rangle$. In a γ^*p collision, these components are included in the $Q\bar{Q}$ -dipole interaction with the proton. In an electroproduction on a nucleus, such multi-gluon fluctuations contribute to the amplitude $\mathcal{A}_{\bar{Q}Q}^N(\vec{r}, x, \alpha, \vec{b})$ in the eikonal formula (5) for the dipole-nucleus amplitude.

At small photon energies, we expect the *Bethe-Heitler regime* of radiation, when each of multiple interactions produces *independent gluon radiation*.

However, the pattern of multiple interactions changes in the regime of long $l_c^{\bar{Q}Qg} \gg d$, where $d \approx 2$ fm is the mean separation between bound nucleons. The gluon radiation length reads

$$l_c^{\bar{Q}Qg} = \frac{2k\alpha_g(1 - \alpha_g)}{k_T^2 + (1 - \alpha_g)m_g^2 + \alpha_g M_{\bar{Q}Q}^2}, \quad (7)$$

where k is the photon energy in the target rest frame, α_g is the LF fraction of the photon momentum carried by the gluon, $M_{\bar{Q}Q}$ is the effective mass of the $\bar{Q}Q$ pair, and $m_g \approx 0.7$ GeV is the *effective gluon mass* fixed by data on gluon radiation [4, 5]. Such a rather large m_g leads to a strong inequality $l_c^{\bar{Q}Qg} \ll l_c^{\bar{Q}Q}$, namely $l_c^{\bar{Q}Qg} = l_c^{\bar{Q}Q}/f_g$, where a large factor $f_g \approx 10$ has been obtained in [6].

At long $l_c^{\bar{Q}Qg} \gg d$, the *Landau-Pomeranchuk effect* is at work when radiation does not resolve multiple interactions acting as one accumulated kick. This leads to a reduction of intensity of gluon radiation compared to the Bethe-Heitler regime. This is why it is called the GS correction.

Thus, the gluon shadowing is part of Gribov corrections corresponding to higher multi-gluon Fock components of the photon and requiring eikonalization of these components. Differently from QQ fluctuations, a QQg component *does not reach* the “frozen” size regime due to the divergent $d\alpha_g/\alpha_g$ behavior. The corresponding variation of the $\bar{Q}Q-g$ dipole size was taken into account adopting the *Green function technique* [2, 7].

The $Q\bar{Q}g$ Fock state is characterized by *two scales*:

(i) One scale determines the small $\bar{Q}Q$ separation, which is $\approx 1/m_Q$ and represents a *higher twist effect*. At large m_Q , it can be treated as a point-like color-octet system; (ii) The second scale determines a much larger $\bar{Q}Q-g$ transverse size.

Thus, the $\bar{Q}Q-g$ system is *strongly asymmetric* and controls GS, which is the *leading twist effect* since is hardly dependent (only logarithmically) on the m_Q . It can be treated with high precision as *glue-gluon dipole* [4] with the transverse size $\approx 1/m_g$. The gluon shadowing factor R_G has been calculated as a function of b_A and rapidity y adopting the Green function formalism. The corresponding values of R_G can be found in Fig. 1 of Ref. [2].

4. Comparison with data

Model calculations of differential cross sections $d\sigma^{\gamma\text{Pb}\rightarrow J/\psi(1S)\text{Pb}}/dt$ and $d\sigma^{\gamma\text{Pb}\rightarrow\psi'(2S)\text{Pb}}/dt$ including effects of $\vec{b}-\vec{r}$ correlation, quark, and gluon shadowing are presented in Fig. 2 [2]. One can see good agreement of our predictions with ALICE data [8]. Predictions for other heavy quarkonium states $\Upsilon(1S)$ and $\Upsilon'(2S)$ can be found in [2].

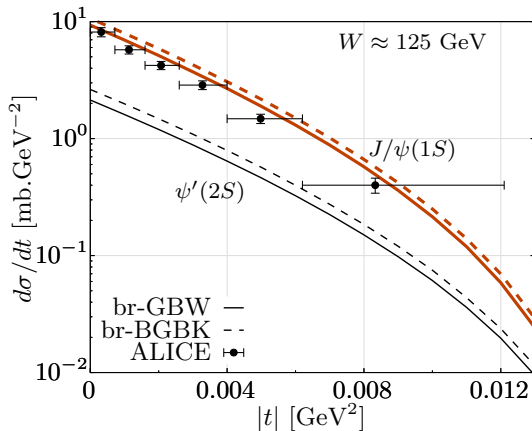


Fig. 2. Predictions for $d\sigma^{\gamma\text{Pb}\rightarrow V\text{Pb}}/dt$ in comparison with ALICE data [8] at $W \approx 125$ GeV.

5. Coherence length for multi-gluon components

The virtual photon with energy k develops a $\bar{Q}Q$ fluctuation for a lifetime

$$l_c^{\bar{Q}Q} = \frac{2k}{Q^2 + M_{\bar{Q}Q}^2} = \frac{1}{xm_N} P_q = l_c^{\max} P_q, \quad (8)$$

where the $\bar{Q}Q$ -effective mass squared $M_{\bar{Q}Q}^2 = (m_Q^2 + k_T^2)/\alpha(1-\alpha)$, so that the factor $P_q = 1/(1 + M_{\bar{Q}Q}^2/Q^2)$. Exact calculations in [6] led to mean values $\langle P_q \rangle_{T,L} \approx 0.36(0.75)$ at $x \sim 10^{-4} \div 10^{-3}$. The inequality $\langle P_q \rangle_L > \langle P_q \rangle_T$ means that L photons develop lighter fluctuations than T ones.

The higher Fock component $\bar{Q}Qg$ has the coherence length

$$l_c^{\bar{Q}Qg} = \frac{2k}{Q^2 + M_{\bar{Q}Qg}^2} = \frac{1}{xm_N} P_g = l_c^{\max} P_g, \quad (9)$$

where the $\bar{Q}Qg$ -effective mass squared $M_{\bar{Q}Qg}^2 = \frac{M_{\bar{Q}Q}^2 + k_T^2}{1-\alpha_g} + \frac{m_g^2 + k_T^2}{\alpha_g} \approx M_{\bar{Q}Q}^2 (1 + \frac{\gamma}{\alpha_g})$ with $\gamma = 2m_g/M_{\bar{Q}Q}^2$, giving thus the factor $P_g = \alpha_g/(\alpha_g + \gamma)$. Averaging P_g over the gluon radiation spectrum $d\alpha_g/\alpha_g$ and fixing the $\bar{Q}Qg$ transverse separation at the mean value $1/m_g$, we obtain $\langle P_g \rangle / \langle P_q \rangle = 0.12$.

For the $|\bar{Q}Q2g\rangle$ Fock state the effective mass squared $M_{\bar{Q}Q2g}^2 \approx M_{\bar{Q}Q}^2 (1 + \frac{\gamma}{\alpha_{g1}} + \frac{\gamma}{\alpha_{g2}})$ and the factor $P_{2g} = \alpha_{g1}\alpha_{g2}/(\alpha_{g1}\alpha_{g2} + \gamma\alpha_{g1} + \gamma\alpha_{g2})$. Performing the averaging process over radiation spectra $d\alpha_{g1}/\alpha_{g1}$ and $d\alpha_{g2}/\alpha_{g2}$, we get $\langle P_{2g} \rangle / \langle P_q \rangle = 0.035$. Straightforward generalization for higher multi-gluon photon components leads to strong inequalities, $M_{\bar{Q}Q}^2 \ll M_{\bar{Q}Qg}^2 \ll \dots \ll M_{\bar{Q}Qng}^2$ and $l_c^{\bar{Q}Q} \gg l_c^{\bar{Q}Qg} \gg \dots \gg l_c^{\bar{Q}Qng}$ with corresponding mean values of l_c at the LHC energy as presented in Table 1.

Table 1. Fractions of the coherence length for $\bar{Q}Q$ Fock state related to higher photon components containing a different number of gluons.

	$\langle P_{ng} \rangle / \langle P_q \rangle$	$\langle l_c \rangle$ [fm]
$\bar{Q}Q$	—	120.0
$\bar{Q}Qg$	0.11940	14.2
$\bar{Q}Q2g$	0.03560	4.2
$\bar{Q}Q3g$	0.01630	1.9
$\bar{Q}Q4g$	0.00952	1.1

In heavy quarkonium production in UPC at the LHC, there are *two dominant sources* of shadowing; the higher twist quark and leading twist gluon shadowing related to $\bar{Q}Q$ and $\bar{Q}Qg$ component of the photon, respectively. However, the quark shadowing is suppressed due to large m_Q . Higher Fock states, $|\bar{Q}Qng\rangle$ with $n \geq 2$, have rather small or negligible contributions to shadowing.

The Balitsky–Kovchegov (BK) equation [9, 10] in combination with the eikonal expression (5) assumes that transverse sizes of all photon components are “frozen” during propagation through the medium, $l_c^{\bar{Q}Q}$, $l_c^{\bar{Q}Qg}$, \dots , $l_c^{\bar{Q}Qng} \gg R_A$. This leads to exaggeration of shadowing effects.

Figure 3 [11] represents a relative comparison of the model predictions for coherent t -integrated cross section based on a solution of the BK equation combined with the Green function formalism, $\sigma_{\text{coh}}^{\text{GF}}$, and with eikonal expression (5), $\sigma_{\text{coh}}^{\text{eik}}$. One can see that even at the LHC collision energy ($W = 125$ GeV), the frequently used traditional “eikonal” calculations cause an *overestimation of shadowing effects* by about 20%. The factor d_V rather slowly decreases with c.m. energy W and one needs quite a large $W \gtrsim 500$ GeV in order to use the “frozen” eikonal approximation with a reasonable accuracy. So one can conclude that the BK equation cannot be applied to nuclear targets.

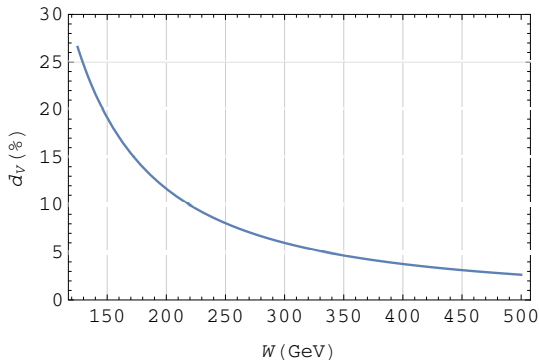


Fig. 3. Relative impact of reduced coherence effects in the BK equation for $\gamma\text{Pb} \rightarrow J/\psi\text{Pb}$ in terms of the energy-dependent factor $d_V(W) = |\sigma_{\text{coh}}^{\text{GF}} - \sigma_{\text{coh}}^{\text{eik}}|/\sigma_{\text{coh}}^{\text{eik}}$.

This work was supported in part by ANID-Chile PIA/APOYO AFB180002. The work of J.N. was partially supported by grant No. LTT18002 of the Ministry of Education, Youth and Sports of the Czech Republic, by the project of the European Regional Development Fund No. CZ.02.1.01/0.0/0.0/16_019/0000778, and by the Slovak Funding Agency, grant No. 2/0020/22.

REFERENCES

- [1] B.Z. Kopeliovich, M. Krelina, J. Nemchik, *Phys. Rev. D* **103**, 094027 (2021).
- [2] B.Z. Kopeliovich, M. Krelina, J. Nemchik, I.K. Potashnikova, *Phys. Rev. D* **105**, 054023 (2022).
- [3] B.Z. Kopeliovich, H.J. Pirner, A.H. Rezaeian, I. Schmidt, *Phys. Rev. D* **77**, 034011 (2008).
- [4] B.Z. Kopeliovich, A. Schäfer, A.V. Tarasov; *Phys. Rev. D* **62**, 054022 (2000).
- [5] B.Z. Kopeliovich, I.K. Potashnikova, B. Povh, I. Schmidt, *Phys. Rev. D* **76**, 094020 (2007).
- [6] B.Z. Kopeliovich, J. Raufeisen, A.V. Tarasov, *Phys. Rev. C* **62**, 035204 (2000).
- [7] Y. Ivanov, B. Kopeliovich, A. Tarasov, J. Hüfner, *Phys. Rev. C* **66**, 024903 (2002).
- [8] ALICE Collaboration (S. Acharya *et al.*), *Phys. Lett. B* **817**, 136280 (2021).
- [9] I. Balitsky, *Nucl. Phys. B* **463**, 99 (1996).
- [10] Y.V. Kovchegov, *Phys. Rev. D* **60**, 034008 (1999).
- [11] B.Z. Kopeliovich, J. Nemchik, «Quantum coherence in the Balitsky–Kovchegov equation», to be published.